

PAC Probes as Diffusion Tracers in Solids

GARY S. COLLINS*, AURÉLIE FAVROT, LI KANG,
EGBERT REIN NIEUWENHUIS, DENYS SOLODOVNIKOV,
JIPENG WANG and MATTHEW O. ZACATE†

*Department of Physics, Washington State University, Pullman Washington 99164, USA;
e-mail: collins@wsu.edu*

Abstract. Perturbed angular correlation (PAC) probe atoms have been used as tracers to study diffusion in solids. The method works for diffusion on a sublattice for which the point symmetry is noncubic and the electric field gradient (EFG) at the probe nucleus reorients in each jump. Such motion leads to relaxation of the nuclear quadrupole interaction. Precise values of the tracer jump frequency have been obtained from fits of measured PAC perturbation functions. Results obtained to date are reviewed for Cd tracer atoms in rare-earth indides such as LaIn_3 that have the L1_2 crystal structure, for which each jump on the In-sublattice reorients the EFG by 90° . New results are presented for LaSn_3 and prospects for future studies are outlined.

Key Words: Cu_3Au structure, diffusion, nuclear relaxation, quadrupole interaction.

1. Introduction

Recently, measurements of the motion of PAC probe atoms, used as tracers, were reported by some of us for compounds having the Cu_3Au structure [1, 2]. These measurements differ from previous studies of nuclear quadrupole relaxation using PAC probes, in which probes were generally at fixed locations with defects hopping in the local vicinity such as lattice vacancies (see, e.g., [3–5]), hydrogen atoms (see, e.g., [6, 7]) or electronic defects (see, e.g., [8]). Those studies were mostly made using probe atoms at sites having cubic point symmetry, so that the electric field gradient (EFG) could be attributed entirely to the neighboring defect. In the present approach, one observes motion of the probe atom itself. For this, the probe must jump on a sublattice of sites having non-cubic point symmetry and the EFG must reorient in each jump. In the experiments reported below, no signals were observed that could be attributed to defects such as lattice vacancies, indicating that the residence time of any such defect next to a probe was much less than the mean residence time of the probe on a site. Thus, only the EFG of the perfect lattice was observed. In this paper, results for ^{111}Cd tracer

* Author for correspondence.

† Present address: Physics and Geology Department, Northern Kentucky University, Highland Heights, KY 41099, USA.

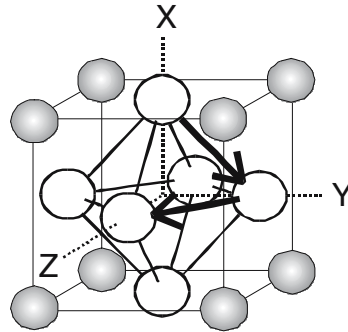


Figure 1. The Cu₃Au (L₁₂) structure, showing tetragonal Cu sites and reorientation of the axis of the EFG from X to Y to Z directions during successive jumps.

atoms jumping on the Cu-sublattice in the Cu₃Au (L₁₂) structure obtained to date are surveyed. Figure 1 shows the crystal structure, with Cu sites having tetragonal symmetry, and it can be seen that the EFG reorients along different (100) cube directions in each jump.

We recently reported on atom movement of ¹¹¹Cd tracers on the In sublattice in LaIn₃ [1] and in other tri-indides formed with Ce, Pr, Nd, Gd, Er and Y [2]. While these phases appear as line compounds in binary phase diagrams, their phase fields must have finite widths, however small. Measurements on LaIn₃ samples purposely prepared with the two phase boundary (PB) compositions exhibited jump frequencies 10-100 times greater at the more In-rich phase boundary than at the less In-rich boundary [1]. Similar results were obtained for CeIn₃ [2]. These results are reviewed and new measurements are presented for Cd tracer motion in LaSn₃ at its two PB compositions. In the discussion, general features of the relaxation method are summarized and prospects for further studies are outlined.

2. Experimental methods

Samples of LaSn₃ were prepared by melting high purity metal foils with ¹¹¹In activity under argon in an arc furnace, after which they were given a crystallizing anneal at high temperature under high vacuum prior to the PAC measurements. Compositions were 23(1) and 28(1) at.% La. The Sn-rich and Sn-poor compositions were selected to produce two-phase samples having a preponderance of Cu₃Au phase and small amounts of neighboring phases. Accordingly, the Cu₃Au phases had compositions at the more Sn-rich and less Sn-rich PBs of the LaSn₃ phase, labeled below as LaSn₃(A) and LaSn₃(B), respectively. As observed also for the indides, inhomogeneous broadening at low temperature was negligible (<0.2 Mrad/s), suggesting that the phases were highly ordered, had low concentrations of thermal or structural point defects, and had PB compositions differing at most by a few tenths of a percent from the stoichiometric composition.

Direct measurements of the boundary compositions were not attempted because no routine method exists for determination of PB compositions to a precision and accuracy of the order of 0.1 at. %.

PAC measurements showed a predominant signal having a quadrupole interaction frequency equal to that previously attributed to ^{111}Cd on the Sn-site in LaSn_3 [9]. (A probe on the cubic La-site would of course have no interaction frequency.) Samples of LaIn_3 and CeIn_3 having the two boundary compositions were prepared in the same way [1, 2]. The remaining indides were prepared with nominally stoichiometric compositions [2], with their actual compositions expected to be at either one or other of the two PBs. PAC measurements were made using a four-counter spectrometer with BaF_2 scintillators, from which PAC perturbation functions $G_2(t)$ were derived [10]. The L1_2 phases exhibit an axially symmetric quadrupole perturbation function which for random polycrystalline texture has the static form

$$G_2^{\text{static}}(t) = \frac{1}{5} + \frac{13}{35} \cos(6\omega_Q t) + \frac{10}{35} \cos(12\omega_Q t) + \frac{5}{35} \cos(18\omega_Q t) \quad (1)$$

at low temperature, in which $\omega_Q \equiv \frac{\pi}{20} |eQV_{zz}|/h$ is the quadrupole interaction frequency. Fitted frequencies were all in excellent agreement with reported values [9]. With increasing temperature, diffusive motion first appears as damping of the static perturbation function. The jump frequency w is defined here as the inverse of the mean residence time of the tracer at a site. Jump frequencies reported in [1, 2] and below were all obtained from direct fits of the measured spectra with perturbation functions computed numerically for a model in which the EFG is axially symmetric and jumps among the three (100) directions. For a description of this fitting method and comparison with various approximate methods, see [11]. Qualitative features of the relaxation are represented well by analytic approximations for PAC perturbation functions given by Baudry and Boyer [12] for a model in which the EFG has constant magnitude, fluctuates among N different orientations, and has an EFG equal to zero when averaged over all orientations. Jumps on the In- or Sn-sublattices fit this model with $N = 3$. In the slow fluctuation regime ($w < \omega_Q$), the perturbation function was approximated by $G_2(t) \cong \exp(-\lambda t) G_2^{\text{static}}(t)$, in which λ is a relaxation frequency. It was found empirically [12] that $\lambda \cong (N - 1)w_{\text{EFG}}$, in which w_{EFG} is the relaxation rate caused by fluctuation of the EFG orientation to a *single* other orientation (note that w_{EFG} is called w in [12]). When the EFG can change to any other orientation in a jump, as in the present diffusion model, the total number of orientations differing from the original one is $N - 1$ and one sees that the total jump frequency is likewise $w = (N - 1)w_{\text{EFG}}$. One thus has the simple result $\lambda = w$. Accordingly, we write for the slow fluctuation regime

$$G_2(t) \cong \exp(-wt) G_2^{\text{static}}(t). \quad (2)$$

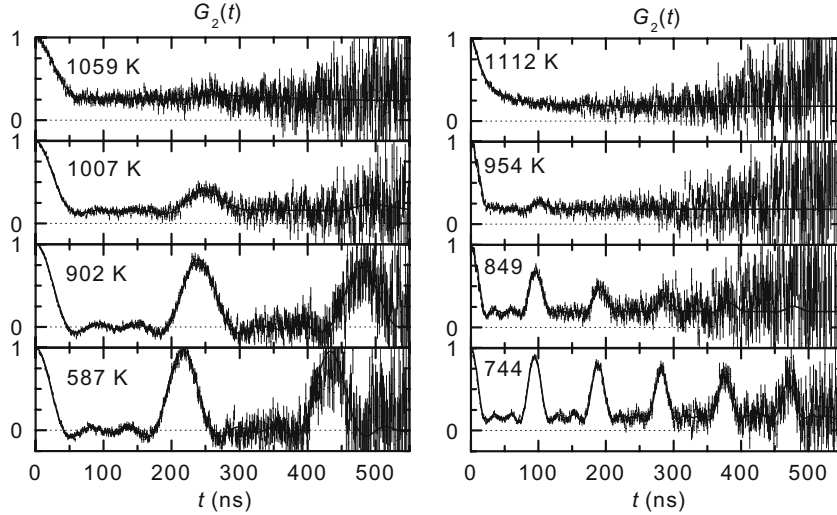


Figure 2. PAC spectra of more Sn-rich LaSn_3 (left) and more In-rich CeIn_3 (right) measured at the indicated temperatures. Increasing relaxation at higher temperatures is attributed to faster jumping of ^{111}Cd tracers on the Sn or In sublattices.

For jump frequencies in the fast fluctuation regime ($w > \omega_Q$), similar consideration of the approximate perturbation function given in [12] leads to

$$G_2(t) \cong \exp\left(-200\omega_Q^2 t / 3w\right). \quad (3)$$

While the damping increases with w in the slow fluctuation regime, it decreases with w in the fast fluctuation regime as a consequence of motional averaging of the EFG. At the highest jump frequencies, the EFG approaches its value averaged over all orientations, which is zero. Note that the actual method used to fit the spectra did not involve approximations such as given by Equations (2) and (3) and excellent fits were obtained also in the intermediate fluctuation regime ($w \approx \omega_Q$). For further information, see [1] and [11].

3. Results

Figure 2 shows effects of relaxation in PAC spectra for ^{111}Cd in Sn-rich LaSn_3 (left) and In-rich CeIn_3 (right). Nearly static perturbation functions observed at low temperatures become increasingly damped at higher temperatures. At high temperatures (1,059 and 954 K), the periodic precessions become completely damped out. Finally, less damping is observed for CeIn_3 at 1,112 K in the fast fluctuation regime. Curves drawn show results of the fits to the exact functions and are in excellent agreement with the data.

Quadrupole interaction frequencies observed at room temperature are in excellent agreement with those listed in [9] and attributed to the Cu_3Au structure.

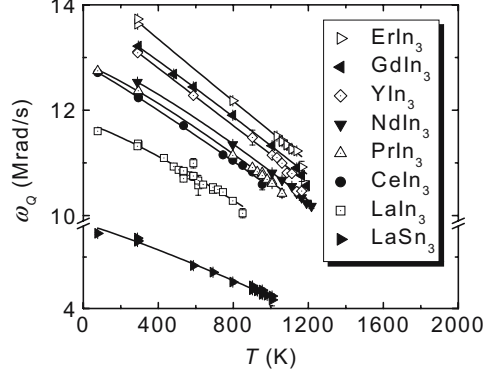


Figure 3. Temperature dependences of quadrupole interaction frequencies for ^{111}Cd probes on the In/Sn sublattices in the indicated compounds. Curves are from fits described in the text.

Table I. Quadrupole interaction parameters and jump frequency activation enthalpies and prefactors for A and B phase boundary compositions

Phase	ω_{Q0} (293 K) (Mrad/s)	B (K^{-1})	ν	PB	Q (eV)	w_0 (THz)
LaSn ₃	5.64 (5)	$2.9 (2) \times 10^{-4}$	1.13 (8)	A	1.22 (5)	$7._{-3}^{+5}$
				B	1.2 (1)	$8._{-6}^{+21}$
LaIn ₃	11.76 (5)	$2.2 (3) \times 10^{-4}$	1.21 (9)	A	0.535 (2)	$1.02_{-0.05}^{+0.05}$
				B	0.81 (1)	$1.4_{-0.2}^{+0.2}$
CeIn ₃	12.86 (3)	$2.1 (1) \times 10^{-4}$	1.08 (4)	A	0.91 (4)	$1.7_{-0.7}^{+1.2}$
				B	1.30 (7)	$11._{-6}^{+13}$
PrIn ₃	12.87 (4)	$2.3 (1) \times 10^{-4}$	1.20 (5)		1.11 (3)	$3.6_{-1.1}^{+1.5}$
NdIn ₃	13.00 (7)	$2.3 (2) \times 10^{-4}$	1.23 (9)		1.80 (5)	450_{-180}^{+290}
GdIn ₃	13.9 (1)	$2.1 (2) \times 10^{-4}$	1.08 (9)		~ 1.2	~ 3
ErIn ₃	14.6 (1)	$1.9 (2) \times 10^{-4}$	0.96 (9)		1.07 (7)	$0.62_{-0.31}^{+0.60}$
YIn ₃	13.9 (2)	$2.0 (2) \times 10^{-4}$	1.00 (9)		1.43 (5)	$34._{-15}^{+26}$

Temperature dependences of the quadrupole interaction frequencies are shown in Figure 3. It can be seen that frequencies in some phases appear to decrease linearly with temperature whereas others decrease more rapidly. Temperature dependences were fitted with the empirical expression $\omega_Q = \omega_{Q0} (1 - (BT)^\nu)$ and values obtained for the quadrupole interaction frequency at 293 K, ω_{Q0} , temperature coefficient B and exponent ν are listed in Table I. All exponents are in the range 1.1(1) and show no obvious systematic trend. Coefficients for the indides are in the range $1.9\text{--}2.3 \times 10^{-4} \text{ K}^{-1}$ whereas a higher value $2.9 \times 10^{-4} \text{ K}^{-1}$ was obtained for LaSn₃.

Figure 4 shows an Arrhenius plot of jump frequencies for all data sets excepting, for clarity, CeIn₃(B) and LaSn₃(B). Each data set exhibits a well defined linear Arrhenius dependence on temperature. Despite similar chemistries, the jump frequencies vary by large factors. Jump frequencies were found to be positively correlated with the lattice parameter in the indides [2]. For both LaIn₃

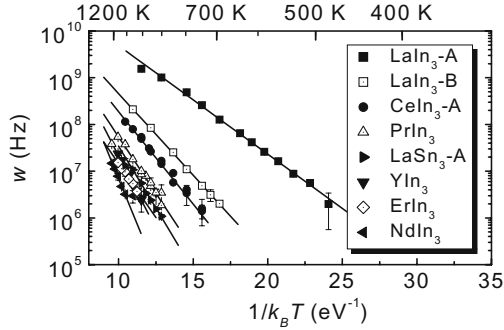


Figure 4. Jump frequencies of ^{111}Cd tracer atoms on the In or Sn sublattices in the indicated compounds.

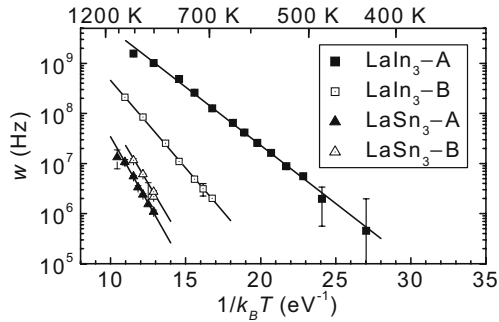


Figure 5. Jump frequencies of ^{111}Cd tracer atoms on the In or Sn sublattices in the indicated compounds.

[1] and CeIn_3 [2], the jump frequency is significantly greater at the In-rich boundary composition.

Figure 5 shows Arrhenius plots for the two LaSn_3 and two LaIn_3 data sets. The jump frequencies can be seen to be greater for LaIn_3 at boundary (A) but for LaSn_3 at boundary (B). Jump frequencies for LaSn_3 are roughly a factor of 10^3 smaller than for LaIn_3 (A). The small factor-of-two ratio between jump-frequencies in the two LaSn_3 samples may indicate that the width of the Cu_3Au phase field in La–Sn is much less than in La–In.

Straight lines drawn in Figures 4 and 5 show results of fits of the jump frequencies for each sample to Arrhenius expressions

$$w = w_0 \exp(-Q/k_B T) \quad (4)$$

in which Q is the jump frequency activation enthalpy and w_0 is a frequency prefactor. Fitted values for Q and w_0 are given in Table I. For LaIn_3 , CeIn_3 and LaSn_3 , separate results are given for boundary compositions that are more In- or Sn-rich (A) and less In- or Sn-rich (B). The values of Q are quite low in these phases. It was shown in [2] that activation enthalpies along the series of indides formed with La, Ce, Pr and Nd are inversely correlated with the lattice

parameter. However, the lattice parameter of LaSn_3 is even greater than for LaIn_3 while the activation enthalpy is also greater, indicating a systematic difference between indides and stannides.

4. Discussion

4.1. DIFFUSION MECHANISMS

The simplest plausible diffusion mechanism is one in which tracer atoms exchange with vacancies jumping freely on the Sn- or In- sublattice, so that the jump frequency is proportional to the concentration of vacancies. However, it can be shown that concentrations of defects such as lattice vacancies on the In or Sn sublattice can only decrease as the composition of In or Sn increases (e.g., see [13]). The simple sublattice vacancy diffusion mechanism therefore can not explain the observation for La- and Ce- indides that jump frequencies were greater for more In-rich samples. On the other hand, the simple mechanism offers a possible explanation for tracer diffusion in LaSn_3 since the jump frequency was smaller for the more Sn-rich sample. Free vacancies in LaSn_3 might occur as structural defects in off-stoichiometric compounds or by thermal activation of an equilibrium defect combination that includes vacancies and preserves the composition. Independent information is needed about defect free energies in these systems in order to interpret the activation enthalpy Q in terms of a diffusion mechanism and enthalpies of formation and migration of point defects.

4.2. FEATURES OF THE PAC TRACER METHOD AND FUTURE PROSPECTS

The jump frequency w is related to the diffusivity D in cubic structures via $D = \frac{1}{6}fw\lambda^2$ [14] in which f is the correlation coefficient of diffusion and λ is the jump distance. The range of accessible jump frequencies depends on the meanlife of the PAC level and for ^{111}Cd is roughly 1–1,000 MHz. This translates to diffusivities in the range 10^{-14} – 10^{-10} m^2/s using the relation between D and w given above and taking $f \approx 1$. From the same relation, it can be seen that the correlation coefficient of diffusion can be determined experimentally from the ratio of measurements of diffusivity and jump frequency carried out using the same tracer.

The nuclear quadrupole relaxation method is incapable of detecting atom movement on sublattices of cubic sites (e.g., in B2 phases) or on sublattices for which jumps lead to no reorientation of the EFG (e.g., in L1_0 phases) because no relaxation is produced. However, there are many sublattices in structures other than L1_2 for which atom movement does lead to nuclear relaxation, for example in the A13 structure of β -Mn [15] and γ -brasses or in the B20 (FeSi) structure. One may also study tracer jumps between inequivalent sublattices for which the magnitude and/or orientation of the EFG changes. Finally, for more complex

structures in which tracer atoms jump on inequivalent sublattices, such as in the B20 structure, one may measure jump frequencies on different sites and determine ratios of inter and intra-sublattice jump frequencies.

Acknowledgement

This work was supported in part by the National Science Foundation under grant DMR 00-91681 (Metals Program).

References

1. Zacate M. O., Favrot A. and Collins G. S., *Phys. Rev. Lett.* **92** (2004), 225901; and *erratum*, *op. cit.* **93** (2004), 49903.
2. Collins G. S., Favrot A., Kang L., Solodovnikov D. and Zacate M. O., submitted to Defect and Diffusion Forum **237–240** (2005), 195.
3. Evenson W. E., Gardner J. A., Wang R. W., Su H.-T. and McKale A. G., *Hyperfine Interact.* **62** (1990), 283.
4. Bai B., Collins G. S., Nieuwenhuis H. T., Wei M. and Evenson W. E., In: Mishin Y., Cowan N. E. B., Catlow C. R. A., Farkas D. and Vogl G. (eds.), *Diffusion Mechanisms in Crystalline Materials*, Materials Research Society Symposium Proceedings **527** (1998), p. 210.
5. Collins G. S. and Nieuwenhuis H. T., *Defect Diffusion Forum* **194–199** (2001), 375.
6. Weidinger A., In: Schlapbach L. (ed.), *Hydrogen in Intermetallic Compounds II*, Topics in Applied Physics, Vol. 67. Berlin, Heidelberg, New York, Springer (1992), 259.
7. Forker M., Herz W., Simon D., Bedi S. C., *Phys. Rev. B* **51** (1995), 15994.
8. Achtziger N. and Witthuhn W., *Phys. Rev., B* **47** (1993), 6990.
9. Schwartz G. P. and Shirley D. A., *Hyperfine Interact.* **3** (1977), 67.
10. Zacate M. O. and Collins G. S., *Phys. Rev. B* **69** (2004), 174202.
11. Zacate M. O. and Evenson W. E., Comparison of XYZ Model Fitting Functions for ^{111}Cd in In_3La , in Proceedings for the HFI/NQI 2004, Bonn, Germany, R. Vianden, ed., unpublished.
12. Baudry A. and Boyer P., *Hyperfine Interact.* **35** (1987), 803.
13. Zacate M. O. and Collins G. S., *Phys. Rev. B* **70** (2004), 24202.
14. Philibert J., *Atom Movements: Diffusion and Mass Transport in Solids* (Les Éditions de Physique, Les Ulis, 1991).
15. Zacate M. O. and Collins G. S., submitted to Defect and Diffusion Forum **237–240** (2005), 396.